J Nanopart Res (2010) 12:2481–2494
DOI 10.1007/s11051-009-9816-6

RESEARCH PAPER

Size-fractionated characterization and quantification of nanoparticle release rates from a consumer spray product containing engineered nanoparticles

Harald Hagendorfer · Christiane Lorenz · Ralf Kaegi · Brian Sinnet · Robert Gehrig · Natalie V. Goetz · Martin Scheringer · Christian Ludwig · Andrea Ulrich

Received: 13 October 2009 / Accepted: 17 November 2009 / Published online: 2 December 2009

Abstract This study describes methods developed for reliable quantification of size- and element-specific release of engineered nanoparticles (ENP) from consumer spray products. A modified glove box setup was designed to allow controlled spray experiments in a particle-minimized environment. Time dependence of the particle size distribution in a size range of 10–500 nm and ENP release rates were studied using a scanning mobility particle sizer (SMPS). In parallel, the aerosol was transferred to a size-calibrated electrostatic TEM sampler. The deposited particles were investigated using electron microscopy techniques in combination with image processing software. This approach enables the chemical and morphological characterization as well as quantification of released nanoparticles from a spray product. The differentiation of solid ENP from the released nano-sized droplets was achieved by applying a thermo-desorbing unit. After optimization, the setup was applied to investigate different spray situations using both pump and gas propellant spray dispensers for a commercially available water-based nano-silver spray. The pump spray situation showed no measurable nanoparticle release,

Electronic supplementary material The online version of this article (doi:10.1007/s11051-009-9816-6) contains supplementary material, which is available to authorized users.

H. Hagendorfer (✉) · R. Gehrig · A. Ulrich
EMPA, Swiss Federal Laboratories for Materials Testing and Research, Ueberlandstrasse 129, CH-8600 Duebendorf, Switzerland
e-mail: Harald.Hagendorfer@empa.ch

R. Gehrig
e-mail: Robert.Gehrig@empa.ch

A. Ulrich
e-mail: Andrea.Ulrich@empa.ch

C. Lorenz · N. V. Goetz · M. Scheringer
ETHZ, Swiss Federal Institute of Technology Zurich, Wolfgang-Paulistr. 10, CH-8093 Zurich, Switzerland
e-mail: Christiane.Lorenz@chem.ethz.ch

N. V. Goetz
e-mail: Natalie.vonGoetz@chem.ethz.ch

M. Scheringer
e-mail: Martin.Scheringer@chem.ethz.ch

R. Kaegi · B. Sinnet
EAWAG, Swiss Federal Institute of Aquatic Science and Technology, Ueberlandstrasse 133, CH-8600 Duebendorf, Switzerland
e-mail: Ralf.Kaegi@eawag.ch

B. Sinnet
e-mail: Brian.Sinnet@eawag.ch

C. Ludwig
PSI, Paul Scherrer Institue, CH-5232 PSI Villigen, Switzerland
e-mail: Christian.Ludwig@psi.ch

C. Ludwig
EPFL, Swiss Federal Institute of Technology Lausanne, CH-1015 Lausanne, Switzerland

whereas in the case of the gas spray, a significant release was observed. From the results it can be assumed that the homogeneously distributed ENP from the original dispersion grow in size and change morphology during and after the spray process but still exist as nanometer particles of size <100 nm. Furthermore, it seems that the release of ENP correlates with the generated aerosol droplet size distribution produced by the spray vessel type used. This is the first study presenting results concerning the release of ENP from spray products.

Keywords Nanoparticle release · Nano-silver · Engineered nanoparticles · Propellant gas spray · Pump spray · Consumer products · SMPS · Electrostatic TEM sampler · Electron microscopy · Image analysis · Environment, health and safety (EHS)

Introduction

Nanotechnology deemed to be one of the most prospective technologies of this century and promises groundbreaking innovation in many application fields. Engineered nanoparticles (ENP) have already found their way into various applications and products. Consumer products containing ENP show a tremendous increase during the past few years. According to a "*Woodrow Wilson International Centre for Scholars*" study on emerging nanotechnologies (2008, available at: http://www.nanotechproject.org), the number of listed consumer products nearly quadrupled, from March 2006 to August 2008. The most common nanomaterial mentioned in the listed consumer products is silver (235 products), followed by carbon/fullerenes (71 products), zinc/zinc oxide (29 products), silica (31 products), titanium or titanium dioxide (38 products), and gold (16 products). In contrast to bulk material, ENP show superior physicochemical properties, related to their small size and large surface area. Chemical composition, surface structure, solubility, shape, and aggregation behavior might be completely different. Nevertheless, the novel properties of ENP also raise concerns about adverse effects on biological systems (The Royal Society 2004). Some studies suggest that ENP are not inherently benign and that they affect biological behaviors at the cellular, sub-cellular, or even protein levels (Borm et al. 2006; Nel et al. 2006; Oberdoerster et al. 2005, 2007). It is suspected that ENP are even too small for defense mechanisms of the body's immune system. Recently, the possibility of non-hindered nanoparticle transfer through the cell membrane directly into cells (Helland et al. 2007; Kaiser et al. 2008, 2009; Wick et al. 2006) has been observed. Studies on the effect of different types of ENP on cell toxicity showed dependency on shape and chemical composition (Brunner et al. 2006; Wick et al. 2007). Exposure of ENP to the human body can occur through the lungs, the skin, or the intestinal tract. In particular, the exposure route via the lungs seems to be very critical due to the large epithelial area of approximately 90–140 m^2. The small size of ENP ensures that a high proportion inhaled from the air reach and deposit in the deep lungs. In consequence, they may pass directly through the cell membrane with the possibility of interfering with important cell functions (Donaldson et al. 1998; Donaldson et al. 2000; Kreyling et al. 2006; Limbach et al. 2007; Nurkiewicz et al. 2008). It was also stated that ENP can pass alveoli membranes and might enter blood streams, where an interference of blood coagulation may be possible, and, therefore, hindering transportation and enrichment, in vitally important organs is possible (Rothen-Rutishauser et al. 2005, 2007).

Several spray products containing ENP are already found on the market. Although exposure via the lung during use is presumable so far, no investigation has been published evaluating the release of ENP from spray products. To the best of this author's knowledge, only exposure to pesticides and other hazardous chemicals to humans via spray applications have been investigated up till now (Berger-Preiss et al. 1997, 2004, 2005, 2006; Class and Kintrup 1991; Gold et al. 1984; Llewellyn et al. 1996; Straube and Bradatsch 2000; Vernez et al. 2006). Hence, the topic of ENP in consumer spray products, especially their implicated exposure scenarios with respect to realistic spray applications using those products, need to be investigated urgently. However, studies on nanoparticle release in aerosols generated by spray products are highly challenging with respect to the experimental setup, reproducible sampling, and reliable analysis. Therefore, techniques which deliver online information on particle size distribution, particle mass and number concentration, as well as elemental composition and morphology are needed.

The most common method for the determination of elemental composition of aerosol particles is by the use of sampling procedures on filters using single-stage impactors (Gehrig et al. 2007; Hueglin et al. 2005; Viana et al. 2008). Such impactors tend to cover the respiratory (<10 μm), the thoracic (<2.5 μm), and the alveole (<1 μm) aerosol fractions. The elemental composition of the collected aerosols can be analyzed by X-ray spectrometry techniques (e.g., X-ray fluorescence spectrometry XRF) or microwave-assisted acid digestion followed by analysis via inductively coupled plasma mass spectrometry (ICPMS), inductively coupled plasma optical emission spectrometry (ICPOES), or graphite furnace atomic absorption spectrometry (GFAAS). For the determination of organic compounds or anions, a preceding extraction step followed by analysis with chromatography techniques coupled to mass spectrometry, conductivity, fluorescence, or UV detection is commonly adopted. Although these methods are well established, time and size resolution is not sufficient to study ENP. Even particle-sampling devices developed for short-time sampling, such as the so-called rotating drum impactor (Bukowiecki et al. 2005, 2007) are limited in size resolution to the above mentioned bulk fractions of 10, 2.5, and 1 μm. The so-called multi-stage or cascade impactors such as an electrical low pressure impactor (ELPI) provide better size resolution down to the nanometer range (Keskinen et al. 1992; Van Gulijk et al. 2000). With an ELPI, for example, particles are sampled in 13 fractions from 10 μm to 30 nm with additional information on particle mass and number concentration. Subsequent elemental analysis, e.g., by ICPMS after microwave acid digestion, provides chemical information (Ulrich and Wichser 2003). However, only three fractions of 13 cover the range of interest below 100 nm for nanoparticle investigations. Moreover, since a minimum particle mass is required for sufficient subsequent elemental analysis, an ELPI is of limited use for short-time events such as the planned spray experiments.

The most promising sampling devices for single particles with subsequent elemental analysis seem to be the electrostatic samplers (Dixkens and Fissan 1999; Fierz et al. 2007a; Liu et al. 1967; Morrow and Mercer 1964). The principle of this method is based on deposition of particles according to their high electrical mobility. The polydisperse and multi-charged aerosol first passes a corona charger; afterward, the now uniformly charged aerosol particle is introduced head-onto a high tension electrode with an above positioned TEM grid, on which the particles are deposited. Subsequent electron microscopy analysis with scanning electron microscopy (SEM) or transmission electron microscopy (TEM) using energy dispersive X-ray spectroscopy (EDX) allow to study individual particles (Kaegi and Gasser 2006; Kirchner et al. 2009; Leppard 2008; Lorenzo et al. 2006) with respect to particle size, morphology, and chemical composition. With the application of imaging analysis software techniques, even particle counting by size is possible. However, in order to sample enough particles for subsequent analysis on size distribution, appropriate sampling times usually between 20 and 120 min are required. Size distribution information with better time resolutions can be achieved by online techniques such as a scanning mobility particle sizer (SMPS) (Agarwal and Sem 1980; Knutson and Whitby 1975; Lehmann et al. 2003; Sioutas et al. 1999). The SMPS basically comprises a differential mobility analyzer (DMA), which realizes a size separation of particles based on electrical mobility, followed by a CPC (condensation particle counter) which counts the fractionated particles. A SMPS electropherogram can typically be obtained within a minimum of 120 s for a size range from 10 to 500 nm. Information on single size classes is also possible within shorter time frames. An even better time resolution can be achieved by the so-called fast mobility particle sizer (FMPS) (Olfert et al. 2008). Commercially available FMPS instruments are able to determine particles in diameters from around 6 to 500 nm with a minimum time resolution of about 1 s. Smaller particle fractions lower than 5 nm are only accessible with the so-called neutral cluster and air–ion spectrometer (NAIS) (Asmi et al. 2008). Furthermore, other fast techniques, such as an electrical diffusion battery (EDB) and the diffusion size classifier (DiSC), cover particle distribution in a size range between 10 and 300 nm with a time resolution down to 1 s. In such instruments, the entering particles are charged in a unipolar diffusion charger by a positive corona discharge and detected with fine wire meshes equipped with sensitive current amplifiers to measure the deposition of the charged particles. However, all the named online particle size techniques are not capable of distinguishing between different particle

types and do not provide chemical information. Therefore, we decided to apply an SMPS in parallel to an electrostatic sampling unit and subsequent electron microscopy analysis, thereby allowing size distribution and information on element composition and morphology of ENP to be achieved at once. In addition, in order to exclude external influences, a sampling environment with minimized particle background is needed to ensure reliable, reproducible, and repeatable data during the simulation of quasi-realistic spray situations.

The developed setup was optimized for quantitative and elemental-specific analysis of particle release from ENP containing spray products, as well as for the investigation of transformation processes in the aerosol. The optimization and spray simulation experiments were performed with a commercially available nano-silver spray product in comparison to a nanoparticle-free spray solution. The two most common spray types—a propellant gas spray and a pump spray—were investigated. This study is the first study on the release of ENP from consumer spray products. The obtained data will be used to model exposure scenarios and evaluate possible risks due to nanoparticle-containing spray products. In future, the setup should become a reliable method to investigate the release of ENP from different spray products. Furthermore, it is planned to adapt this setup so that it can be used also for the studies of abrasion release processes.

Experimental

For this study, a commercially available water-based nano-Ag spray product and the related nanoparticle-free blank solution were investigated. The producer specified a silver concentration of 1,000 mg/L with a mean particle size of 26 nm determined by dynamic light scattering. The particles are produced in a bottom-up process and stabilized with $NaHCO_3$. Berger-Preiss et al. (2005) mentioned a significant influence on the nozzle type during spray experiments for biocides. In order exclude this influence, refillable dispensers were chosen to ensure comparable conditions for every spray experiment. The producer provided two types of spray dispensers—a pump spray dispenser (0.5-L volume made of Polyethylen)

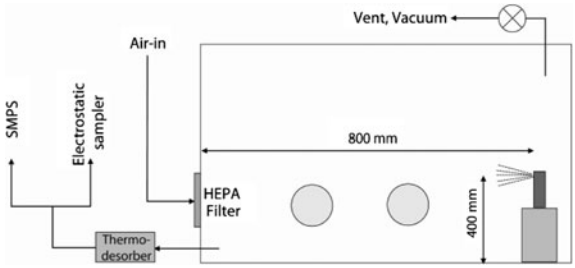

Fig. 1 Scheme of the setup used for the spray experiments

and a propellant gas spray dispenser (PREVAL Spray Gun, Haubold Technik, Moerlenbach, Germany) with a mixture of dimethyl-ether, iso-butane, and propane as a propellant gas. All the spray experiments were carried out exactly at the same position, and the spray nozzle was always adjusted to the same height (see Fig. 1). The filled spray dispensers were weighed before and after every spray event to determine the amount of sprayed solution.

Bulk analysis

For total element analysis of the nanosilver dispersions, acid microwave digestion with subsequent ICPMS analysis was applied. From a homogenous, yellowish Ag-nanoparticle dispersion, 0.5 g was transferred to quartz microwave vessels, and 5 mL of 65% nitric acid (suprapur, Merck, Darmstadt, Germany) was added. After microwave digestion (220 °C, 30 min), a clear solution was obtained. The digest was transferred to PE vessels and filled with 18 mΩ cm DI water (Milipore AG, Zug, Switzerland) to 50 mL. The analysis was carried out on an Agilent 7500ce ICPMS (Agilent Technologies, Waldbronn, Germany) using an external calibration adjusted against Rh as internal standard. For the size distribution analysis of the nano-Ag particles, the spray dispersion was centrifuged onto formvar/carbon-coated mesh 200 copper grids (SPI #3420C, SPI Inc., West Chester, PA, USA) (Lienemann et al. 1998). Imaging was done on a FEI Morgagni TEM (FEI, Hillsboro, Oregon, USA) with a tungsten filament and 100-kV acceleration voltage. Particles were counted using image analysis software (Adobe Photoshop CS® with Image Processing Tool Kit, Reindeer Games Inc., Asheville, NC, USA).

Aerosol spray analyses

Figure 1 shows a scheme of our measurement setup. In ooder to achieve a particle-minimized environment, a commercially available plexiglass glove box (Meca-Plex, Grenchen, Switzerland) with dimensions of 94 × 55 × 67 cm (b, l, h,) and a total volume of 300 L was modified. The glove box was equipped with an exhaust and a vacuum junction for fast particle evacuation. A ventilation system with a capacity of 1,000 m^3 per hour and an additional siphon connection ensured a rapid air exchange in the glove box. In order to guarantee a minimal particle environment inside the glove box, the aspirated air was directed through a double layer of HEPA filters (HS-Mikro SF AL, HS-Luftfilterbau GmbH, Germany). Shortly before and during spray experiments, the siphon and vent were switched off until atmospheric pressure was achieved prior to the measurement.

All instrument tubing connections were made of Tygon® with an inner diameter of 5 mm. The aerosol flow leaving the glove box was first directed through a low flow thermodesorber (Fierz et al. 2007b) to dry the aerosol. After the thermodesorber, the flow from the glove box was divided into two streams using a T-junction: One was directed to a SMPS (TSI, model 3034, TSI GmbH, Aachen, Germany), and the second to an electrostatic sampler designed by Fierz et al. (2007a).

Both tubing connections between T-junction and SMPS and electrostatic sampler, respectively, had similar lengths. Operating the two devices in parallel allowed a direct comparison of particle number concentrations and size distributions from the same spray experiment and the same time interval. The SMPS was used for online quantification of the particle release. The measurement interval was not adjustable and fixed at 10–500 nm with 32 channels per decade and 1 scan per sample. As a consequence, the measurement time was 3 min. The electrostatic sampler used was capable of sampling the released particles on TEM grids. Subsequent analysis using electron microscopy techniques allowed chemical and morphological characterization and validation of the SMPS measurements. Addition, the sampler was already calibrated according the deposition efficiency over size (silver particles from 20 to 330 nm). For smaller particles, the calibration function was extrapolated. For quantification of the electrostatic sampled particles, four images from the center of the TEM grid were analyzed. The particles were deposited on formvar/carbon-coated-200 mesh copper TEM grids (SPI #3420C, SPI Inc., West Chester, PA, USA). For microscopy analysis, a Hitachi S-4800 SEM (Hitachi High-Technologies Europe GmbH, Krefeld, Germany) equipped with an EDX unit was available (15 kV for EDX, 1 kV for imaging). Particle counting was performed with image analysis of the derived SEM images (Adobe Photoshop CS® with Image Processing Tool Kit, Reindeer Games Inc., Asheville, NC, USA). The images were processed as follows: set to grayscale mode/set threshold values/erode (coeff.: 1, depth: 2)/fill holes/measure all the features. In order to obtain the particle number concentration first, correction according to the size dependence and subsequent extrapolation of the particle numbers to the complete deposition area of the electrostatic sampler was performed. Operation, calibration, and tuning of the electrostatic sampler and the thermodesorber are described elsewhere by other authors (Fierz et al. 2007a, b).

Results and discussion

Analytical part

Bulk analysis

Prior to the characterization of ENP released during the aerosol-generated spray process, a chemical and morphological characterization of the nano-Ag dispersion and the nanoparticle-free spray solution was performed. In the nanoparticle dispersion, a concentration of 1040 ± 60 mg Ag/L ($n = 3$) was determined. The results correspond well with the specification of the manufacturer of 1,000 mg Ag/L. In the nanoparticle-free spray solution, Ag was not detectable. The TEM images of the centrifuged nano-Ag dispersion show an in-homogenous distribution of the particles with partly aggregated clusters (Fig. 2). The aggregated particle clusters were determined in a size range of 20–100 nm, but single particles are clearly distinguishable. The aggregation might be a result of sample preparation by centrifugation. Therefore only the single particles were counted. The image analysis resulted in a main narrower size mode of 6 nm, and a second, broader size fraction of size

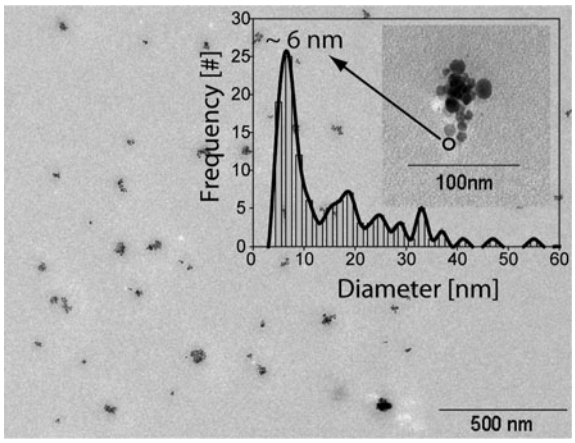

Fig. 2 Bulk particle distribution: TEM image after centrifugation of the nano-silver dispersion on a carbon-coated copper TEM grid and the related size distribution obtained by image analysis

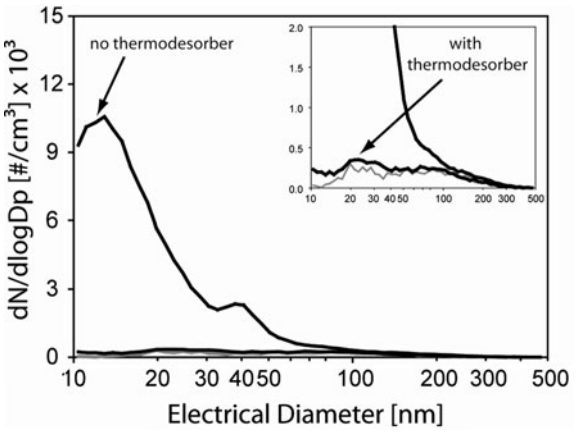

Fig. 3 Comparison of the SMPS signals of the nanoparticle-free solution sprayed for 1 s with the propellant gas spray dispenser measured by SMPS without and with prior drying in the thermodesorber (*black lines* signals for the sprayed aerosol, *gray line* glove box background before the spray event)

range 15–60 nm. On the images of the nanoparticle-free spray solution, particles were not detected.

Glove box setup

Reliable measurement of release rates from spray products requires a simulation of spray situations, favorable with online analysis of the emitted particles. Moreover, defined conditions for the spray experiments are mandatory for comparable data. Thus, a closed environment with minimal particle background is needed to perform the spray experiments. The closed glove box setup ensured stable conditions and avoided incalculable influences such as air flows. The setup used assured a minimal particle background environment with maximum of 500 particles per cm^3 in the measured size range between 10 and 500 nm for the sprays. The particle evacuation after a spray experiment required around 20 min of flushing the glove box till reaching acceptable background levels.

Spray experiments

In a first attempt, the particle distribution was measured with SMPS immediately after a spray experiment. The aerosol of the nanoparticle-free spray solutions generated with the propellant gas spray bottles resulted in a measurable SMPS signal between 10 and 30 nm (see Fig. 3), whereas the experiment in pump spray dispensers show no significant difference to the glove box background. Since a differentiation between wet and solid particles by SMPS is not possible, the signal is probably caused by nano-sized droplets formed by the propellant gas spray process. In order to prove this assumption and measure the solid particles only, a low-flow thermodesorber was applied to dry the aerosol prior to determination. Figure 3 shows a comparison of the propellant gas spray nanoparticle-free solution measured with and without thermodesorber. For the dried aerosol of the nanoparticle-free solution using a thermodesorber prior to SMPS measurements, almost the same low particle number as the glove box background was achieved. The results obtained let us assume that probably nano-sized aqueous droplets are responsible for the SMPS signal when spraying the nanoparticle-free solution.

Figure 4a presents the results of three distinct SMPS scans, after a spray experiment (1 s spray time) with the propellant gas spray dispenser. The size profile points out, that after 3 min, the particle number concentration decreased to about a third of the level achieved directly after spraying, but is still larger than the initial background level. Hence, it can be assumed that due to particle coagulation, deposition and loss in the glove box, the particle concentration reduces very rapidly. The difference of the particle distribution measured from the 3rd to 6th min (measurement cycle 2), after the spray event, is only

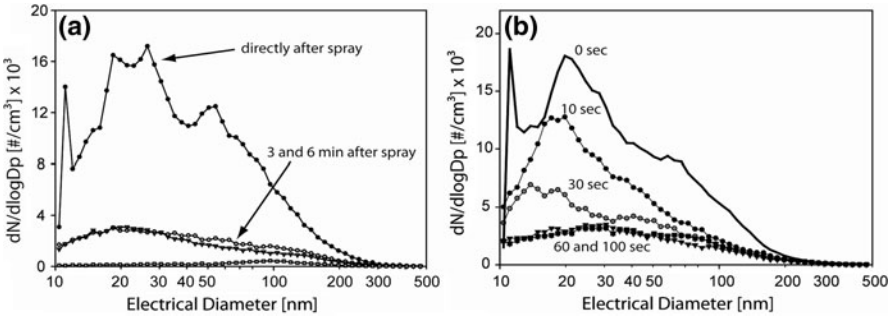

Fig. 4 **a** SMPS electropherograms of a spray experiment with the propellant gas spray dispenser and the nano-silver dispersion (**a**); (•) directly after the spray event, (•) 3 min after spray event, (▼) 6 min after spray event, and (■) background before measurement. **b** Time dependence of the particle size distribution: Start of the SMPS data acquisition 0 (–), 10 (•), 30(◉), 60 (■), and 100 (▼) seconds after the spray event. All the data are normalized to weighed spray amount per experiment

slightly smaller than the following one (measurement cycle 3). This situation did not change for a period more than 30 min. Nevertheless, even with the observed particle loss right after the spray experiments, the concentration still is approximately a factor 10 higher than the background.

In order to get a better understanding of the observed particle loss, it is desirable to observe fast processes such as coagulation and particle growth after the spray experiment. Since different size classes are sequentially measured by SMPS, a full scan over the selected size range, i.e., from lowest to the highest size class, requires 3 min of measuring time. In fact, this prohibits a proper observation of the fast processes occurring right after the spray experiments. Unfortunately, simultaneous instruments such as the FMPS which have faster acquisition times, were not available for this project. At least to get an idea how fast the particle loss emerges, we changed our sampling strategy for the SMPS. Therefore, the spray experiments were performed with shifted start times of the SMPS (0, 10, 30, 60, and 100 s after the spray event) to determine the observed time dependence of the particle distribution. Since an SMPS usually scans from the lowest to the highest size class, this method allows a data acquisition for specific size classes at different times.

However, a prerequisite for measurements with shifted start times is good reproducibility of spray experiments. Reproducibility of the developed setup was validated by repetition of spray experiments with the water-based nano-silver spray dispersion in a propellant gas spray dispenser. Each spray experiment was repeated three times independently. Before each experiment, the glove box was flushed and evacuated, until background levels below 500 particles/cm^3 were reached. Each measurement was carried out immediately after a spray experiment with a spray time of 1 s. The amount of sprayed dispersion was determined by weighing the dispenser before and after each spray experiment (0.68 ± 0.02 g, $n = 3$). The SMPS electropherograms directly after the spray experiments slightly differ in size distribution and show two or three modal distributions. Furthermore, in all the first size scans, the edge of a peak is visible with a maximum of around 10 nm. Two of the three scans show also a third peak at larger size fractions of 50 or 60 nm, respectively, which could be an indication for starting aggregation or agglomeration processes. The main peak appears at a maximum of around 25 nm for all the three spray experiments. However, the total number of the particles (sum of all the particles between 10 and 500 nm) is constant at $18{,}700 \pm 1{,}300$ per cm^3 ($n = 3$, normalized to the sprayed amount), which corresponds to a relative standard deviation of 7%. The electropherograms after approximately 60 s, when a stable condition is reached, show only one single and broad peak of much lower intensity. A fewer variations of the size distributions were observed, and the total number of particles between 10 and 500 nm was determined to be 3500 ± 100 partilces per cm^3 ($n = 3$, normalized to the sprayed amount), which corresponds to a relative standard deviation of 2.8%.

Figure 4b shows the SMPS electropherograms obtained by shifting the starting time of the

measurement. After about 60 s, the situation in the glove box did not change any further. It is obvious, directly after the spray event, that particle distribution and concentration differ and that particle loss occurs in the timescale of several seconds. The particle distribution measured right after the spray event shows three particle size modes at 12, 24, and 60 nm electrical diameter comparable to the reproducibility experiments. Shortly after (<10 s) the spray event, the peak at 12 nm disappears. With increasing time (10–30 s) after the spray event, the highest (60 nm) particle size mode also disappears, and the middle mode shifts to smaller electrical diameters. After 60 s, only one, very broad particle size mode that shifted again to higher electrical diameters can be observed.

Since the original dispersion contained two size classes of ENP, one with a maximum of around 6 nm and the other with a maximum at around 30 nm (Fig. 2), the edge of the smallest peak could be interpreted as follows: In the very first few seconds after the spray event, still primary particles released from the dispersion are present. Within the first 10 s, the small primary particles possibly driven by aggregation or agglomeration form larger clusters. Thereafter (10–30 s), it seems as though a series of agglomeration processes of the small primary particles as well as adhesion of larger particles to the glove box walls or floor take place. After 100 s, a stable particle size distribution is present, but still shows a major amount of particles smaller than 100 nm.

Quantification strategies

The fact that particle loss occurs, which results in time dependency of the particle distribution, makes an exact quantification of total particle numbers challenging. If only the particle distribution right after the spray event is taken into account, it results in a worst-case scenario. Considering only the size distribution of the stable condition in the glove box possibly reflects long-term exposure. In order to assure the data obtained by SMPS and to gather morphological and chemical information, we decided to use an electrostatic TEM sampler. Thus, deposition of particles on a TEM grid and consequent electron microscopy analysis deemed itself quite reliable. Furthermore, size-dependent deposition rate calibration of the sampler and the use of image analysis software allowed us to quantify the particles and compare it with the data obtained by SMPS. Nevertheless, for particle counting with image analysis, a reliable and homogenous particle loading on the TEM grid to minimize statistical error is essential. Thus, a measurement of spray events in series was performed to optimize the sampling procedure. The goal was to obtain a statistical by sufficient number of particles per image at appropriate magnifications with minimized sampling times. Furthermore, homogenous distribution over the TEM-grid is desired. This was proven by counting ten segments along a profile of a sampled TEM grid. A collection time of 1 h (20 SMPS measuring intervals) with seven spray events each following two subsequent stabilization intervals was found to be appropriate to achieve reliable particle counts. Figure 5a shows a typical SEM picture (inverted grayscale), which was used for data processing using the image analysis software. With the optimized sampling procedure, the deposition of approximately 50 particles per analyzed image (20 k× magnification) was achieved for spray experiments with the propellant gas spray and the nano-silver dispersion. Figure 5b shows the results of the particle distribution on the TEM grid. Investigation of the particle number was done across ten single meshes dislocated over the TEM grid. Every data point consists of a mean and standard deviation of counted particles of four images in the same segment (40 images in total). The particle load over the TEM grid shows a mean particle number of 44 ± 8 which represents a relative standard deviation of 18%.

Results part

Particle release by propellant gas or pump

In order to determine and quantify the particle release rates and to obtain chemical and morphological information, the above described setup was used for the investigation of both–an aerosol of the nano-silver spray product generated by a propellant gas spray and by a pump spray dispenser. All the spray experiments were initially performed with the thermodesorber to collect the solid particles only. Afterward, the experiments were repeated without the thermodesorber to determine its influence on the particle size and quantity. Furthermore, the same sampling

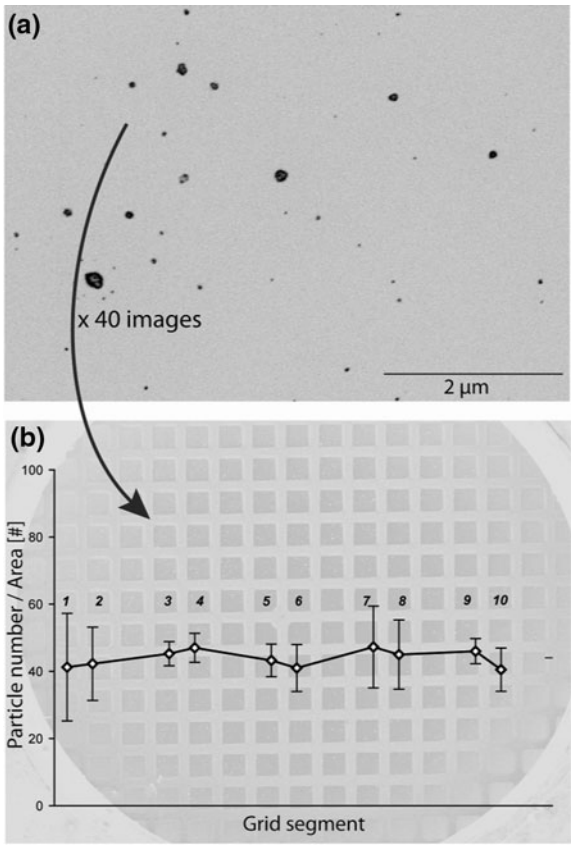

Fig. 5 **a** Typical inverted SEM image (negative mode) of the nano-silver particles, collected with the electrostatic sampler during spray experiments using the propellant gas spray dispenser. **b** Profile of the counted particles over a TEM grid. *The diamonds* represent the particle number concentration detected on the corresponding TEM grid segments. Every data point consists of a mean and standard deviation of the counted particle obtained form four images in each segment area which corresponds to 40 images in total. A part of the grid was covered by the grid holder

procedure was performed using holey carbon-coated copper TEM grids for chemical characterization of the particles through EDX.

Figure 6 shows the comparison of the particle number distribution obtained by SMPS and the electrostatic sampler of the propellant gas spray experiment for nanosilver sprays. Figure 6a shows three curves, representing the size distribution determined by SMPS: (I) only as a mean of the stable condition, (II) as a mean of all events during the first hour of sampling (blank and seven spray events including two subsequent measurement after each spray event), and (III) as a mean of the situation directly following the spray event. As already discussed, the profile (III) represents a kind of worst-case scenario whereas profile (I) can be considered as a long-term-exposure scenario.

Figure 6b shows the particle size distribution determined with the electrostatic sampler of the same spray experiments. It fits well with the SMPS data taking into account only the stable condition (I) which shows the peak maximum and particle concentrations in the same range of around 25 nm. The size distribution of the SMPS data considering all spray- (II) and "after spray" (III) situations also show a comparable size distribution. Although the SMPS shows the same peak maximum at around 25 nm comparable to the peak maximum of the electrostatic sampler, a significant higher particle number concentration (Table 1) was obtained. Owing to the necessarily long sampling time (60 min) of the electrostatic sampler, the determined particle distribution has a different time resolution compared to that of the SMPS data. Although the electrostatic sampler should accumulate also the higher concentrations of particles immediately after the spray experiments, the long sampling time of 60 min represents the more stable condition obtained by SMPS. In theory, the particle concentration obtained by the electrostatic sampler should be somewhere in between the stable condition and the situation right after the spray event. Probably because deposition rates were not verified for particles smaller than 20 nm (calibration function of particles $<$20 nm is extrapolated); the particle concentration is underestimated compared to the SMPS. A further indication for this assumption is that the particle distribution between 10 and 20 nm determined by the electrostatic sampler shows a steeper fall off compared to the SMPS. Furthermore, a homogenous distribution of particles over the entire TEM grid is less granted with reducing particle size. Therefore, under- or overestimations can occur if only outer or inner segments are analyzed and counted.

Figure 7a shows an EDX spectrum of one sampled aerosol particle (sampled on holey carbon copper TEM grids) which was generated during the spray experiment for the nanosilver dispersion with the propellant gas spray dispenser. The spectrum shows signals for O, Na, and Ag which can be clearly assigned to the nano-Ag dispersion particles emitted during the spray process. The silver nanoparticles in the solution were produced by the so-called bottom-up

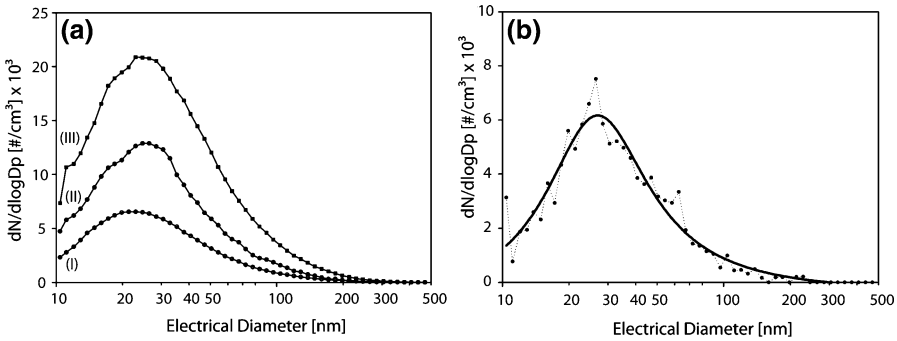

Fig. 6 Comparison of the size distribution using a propellant gas spray dispenser with the nano-silver dispersion. All the data were obtained with **a** SMPS or **b** electrostatic sampler with subsequent electron microscopy analysis and image software-supported particle counting. The curves in the SMPS graph (**a**) represent (I) all the spray events including stable condition and blank, (II) the mean of the stable condition only, and (III) the mean of the "after spray" only, which represents the worst-case scenario

Table 1 Calculated particles release rates sampled during spray experiments using a propellant gas spray and a pump spray dispenser

Method	Sprayed amount/time (g/h)	$dN/cm^3 < 100$ nm (#/cm^3)	Peak max (nm)
Propellant gas spray			
SMPS I (stable condition)	4.94	3300 ± 400	23
SMPS II (all events)		8000 ± 1000	25
SMPS III (after spray)		14000 ± 2000	25
Electrostatic sampler		3800 ± 700*	26
Pump spray			
SMPS	4.20	n.d.	n.d.
Electrostatic sampler		n.d.	n.d.

n.d. not detectable

* The standard deviation of 18% was calcualted from TEM grid allocation experiment

process by reduction of a silver nitrate solution and then stabilized using $NaHCO_3$. The EDX signal for Cu is probably caused by the carbon-coated copper TEM grid itself.

A comparison of the particle size distribution of the aerosol and the original dispersion shows that the particles in the dispersions seem to be smaller in diameter than the released particles especially after a certain aging of the aerosol. Figure 7b shows the magnification of a silver cluster of approximately 200 nm in diameter found deposited on a TEM grid in the electrostatic sampler. The morphology of this particle gives reason to assume that the agglomeration of small silver particles take place during the spray process. Several particle clusters of the same form and shape and having various sizes were observed in the propellant gas spray dispenser experiments for the nano-silver spray. Most of the clusters were smaller than 100 nm.

This finding leads to the assumption that the particles are homogeneously distributed in the single spray aerosol droplets while spraying. After spraying, the droplets evaporate, and the particles start to agglomerate. In this case, the use of the thermodesorber unit might support agglomeration and enlargement of particles because it fastens the droplet drying process. In order to further investigate this assumption, spray experiments were performed without drying beforehand in the thermodesorber. Unfortunately in this case, the SMPS was not feasible, due to the high background signal without prior drying of the aerosol in the thermodesorber (see Fig. 3). Thus, particle size distribution was determined using electrostatic sampling. Figure 8 shows some representative

SEM images collected with the electrostatic sampler and the corresponding particle size distribution. With a closer look at the images used for the analysis (Fig. 8b–d), a lot of spherical aggregates with allocated small Ag particles can be found when sampled without prior drying. In the image analysis, those particles are counted as one large sphere. In consequence, the acquired particle distribution shows a higher amount of particles in the area between 50 and 500 nm compared with the results obtained using the thermodesorber.

This, in fact, strengthens our assumption that most of the particles are not transported as free ENP but as particles with a volatile hull (in this case water): The larger the droplets the longer the time for evaporation and agglomeration of the droplets containing Ag nanoparticles. Thus, smaller droplets evaporate fast, and the Ag nanoparticles agglomerates arise which are sampled on the TEM grid. In contrast, bigger droplets do not evaporate fast enough and, in consequence, they are sampled as droplets on the TEM grid, where they then dry up. Further indication for the assumption, that the particles are transported in droplets rather than as free ENP, can be provided by the differing results obtained using a pump spray. In contrast to the propellant gas spray, the SMPS signal for aerosols generated with the pump spray did not show any particle release. Even with the use of electrostatic sampling also no particles could be found on the TEM grid. It is worth mentioning that during the experiments, it was obvious to notice that the pump spray dispenser produces mainly larger droplets, and most of them are deposited on the glove box floor or wall due to gravity, whereas the aerosol generated by propellant gas spray dispensers seem to have a much smaller droplet size distribution. The SMPS experiments during method development

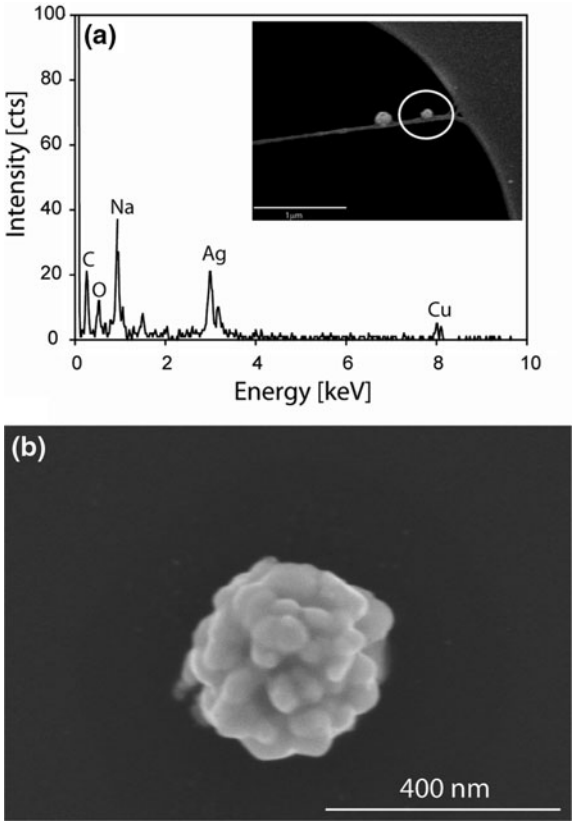

Fig. 7 **a** EDX spectra of a nano-silver particle (~100 nm diameter) sampled with the electrostatic sampler and deposited on a copper coated carbon TEM-grid with holes. **b** SEM image of an agglomerated Ag particle collected with the electrostatic sampler from experiments with the propellant gas spray dispenser

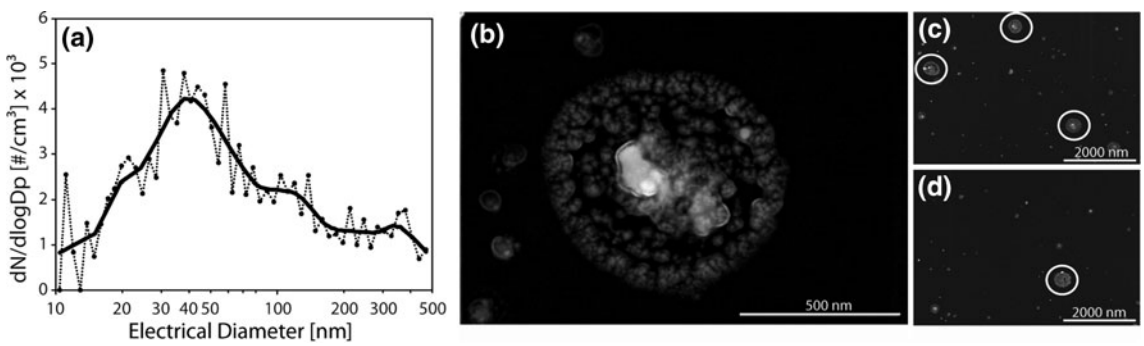

Fig. 8 **a** Obtained particle size distribution by particle counting of the water-based nano-silver spray (propellant gas spray) sampled with the electrostatic sampler without prior drying using the thermodesorber unit. Corresponding SEM images: **b** magnification of Ag particle agglomeration, and **c**, **d** agglomerates counted as one particle by the image-processing software analysis

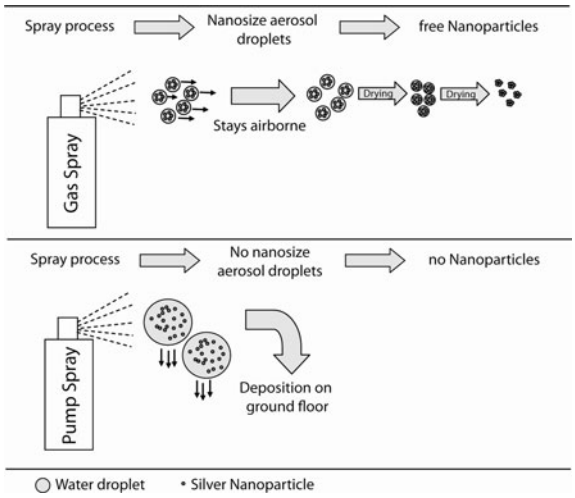

Fig. 9 Scheme of our understanding of the spray process, subsequent nanoparticle transport and release using a propellant gas spray and a pump spray for the aqueous nano silver product

revealed already a droplet fraction even in the nanometer size range when only water was used (see Fig. 3).

In consequence, it can be assumed that for the water-based nanosilver spray dispersion, investigated here the release of the ENP is mainly influenced by the aerosol droplet size distribution generated by the spray type used. In Fig. 9, our understanding of the spray process is shown: with the use of propellant gas sprays, droplets in the nanometer range are evolving from the spray process. The residence time for these droplets in the aerosol is long enough such that the solvent can evaporate. After evaporation of the liquid phase, the nanoparticles in the droplets start to build aggregates still in the nanometer size range. With the use of pump sprays, no aerosol droplets in the nanometer size range can be observed. The droplets are big enough not to remain in the air, but deposition on the glove box wall and ground floor appears. Thus, the arising particles, after evaporation of the solvent, are adhered and cannot be detected in the aerosol anymore.

Conclusion

The used glove box setup is appropriate for a reliable investigation of the release of ENP from spray products in a particle-minimized environment. Information about concentration, elemental distribution, and morphology of the released particles in the range of 10–500 nm was obtained. The method of performance was illustrated on a commercially available nano-silver product for two different spray situations carried out with a propellant gas spray and a pump spray dispenser.

The acquired data by SMPS allowed us to conclude that propellant gas sprays in contrast to pump sprays already release droplets in the nano-size range even if ENP are not present in the spray dispersion. Investigations with a thermodesorber unit proved that these droplets are mainly volatile, and most probably, nano-sized water droplets are produced by the spray process itself. However, solid particles different from the fine aerosol water droplets are released when using propellant gas sprays containing a water-based nano-silver-spray dispersion. In contrast, the aerosol generated by pump spray dispensers seems to form larger droplets which deposit on the glove box floor and walls. Also, ENP release could not be obtained using the pump spray dispenser.

The data obtained with electrostatic sampling confirm the results found with SMPS. Here, the pump spray experiment also did not show any particle release whereas the particle size distribution and total particle concentration for the propellant gas spray were in good agreement with the SMPS findings. Furthermore, the electron microscopy analysis confirms that these particles are of the same origin as the particles in the dispersion, but they differ in size and morphology due to aging of the aerosols leading to agglomeration or aggregation.

Obviously, the release of ENP during the spray process depends on the particle size distribution of the aerosol droplets produced by different spray dispenser types. It seems likely that propellant gas spray dispensers produce water droplets in the nanometer to micrometer size range. These droplets seem to contain the suspended ENP in homogeneous distribution. After the water droplets evaporate (either due to accelerated drying in the thermosdesorber or after wet deposition, e.g., on the TEM grids in the electrostatic sampler), the ENP aggregate and start to build up large clusters, but in diameters which are mainly remain below the toxicologically critical size range of 100 nm (non-hinderance transport across cell membranes).

This finding raises a number of questions also about sprays containing solvents different from water. Most of the sprays found on the market with organic solvents often contain additional perfluorinated compounds. Moreover, due to the finer distribution, propellant gas spray dispensers are more often used than pump sprays. Owing to different surface tensions of organic solvents, it is presumable that the particle distribution of the aerosol droplets is also different. However, further investigations as well as a further development of the method are necessary and will be done to answer these questions.

Acknowledegments The authors would like to thank the FOPH (Swiss Federal Office of Public Health) for funding, especially Steffen Wengert, and also many co-workers not mentioned, for their time and help.

References

Agarwal JK, Sem GJ (1980) Continuous flow, single-particle-counting condensation nucleus counter. J Aerosol Sci 11(4):343–357

Asmi E, Sipila M, Manninen HE, Vanhanen J, Lehtipalo K, Gagna S, Neitola K, Mirme A, Mirme S, Tamm E, Uin J, Komsaare K, Attoui M, Kulmala M (2008) Results of the first air ion spectrometer calibration and intercomparison workshop. Atmos Chem Phys Discuss 8(5):17257–17295

Berger-Preiss E, Preiss A, Sielaff K, Raabe M, Ilgen B, Levsen K (1997) The behaviour of pyrethroids indoors: a model study. Indoor Air 7(4):248–261

Berger-Preiss E, Koch W, Behnke W, Gerling S, Kock H, Elflein L, Appel KE (2004) In-flight spraying in aircrafts: determination of the exposure scenario. Int J Hyg Environ Health 207(5):419–430

Berger-Preiss E, Boehncke A, Koennecker G, Mangelsdorf I, Holthenrich D, Koch W (2005) Inhalational and dermal exposures during spray application of biocides. Int J Hyg Environ Health 208(5):357–372

Berger-Preiss E, Koch W, Gerling S, Kock H, Klasen J, Hoffmann G, Appel KE (2006) Aircraft disinsection: exposure assessment and evaluation of a new pre-embarkation method. Int J Hyg Environ Health 209(1): 41–56

Borm PJA, Robbins D, Haubold S, Kuhlbusch T, Fissan H, Donaldson K, Schins R, Stone V, Kreyling W, Lademann J, Krutmann J, Warheit DB, Oberdorster E (2006) The potential risks of nanomaterials: a review carried out for ECETOC. Part Fibre Toxicol 3:11

Brunner TJ, Wick P, Manser P, Spohn P, Grass RN, Limbach LK, Bruinink A, Stark WJ (2006) In vitro cytotoxicity of oxide nanoparticles: comparison to asbestos, silica, and the effect of particle solubility. Environ Sci Technol 40(14):4374–4381

Bukowiecki N, Hill M, Gehrig R, Zwicky CN, Lienemann P, Hegedues F, Falkenberg G, Weingartner E, Baltensperger U (2005) Trace metals in ambient air: hourly size-segregated mass concentrations determined by synchrotron-XRF. Environ Sci Technol 39(15):5754–5762

Bukowiecki N, Gehrig R, Hill M, Lienemann P, Zwicky CN, Buchmann B, Weingartner E, Baltensperger U (2007) Iron, manganese and copper emitted by cargo and passenger trains in Zürich (Switzerland): size-segregated mass concentrations in ambient air. Atmos Environ 41(4):878–889

Class TJ, Kintrup J (1991) Pyrethroids as household insecticides: analysis, indoor exposure and persistence. Fresenius J Anal Chem 340(7):446–453

Dixkens J, Fissan H (1999) Development of an electrostatic precipitator for off-line particle analysis. Aerosol Sci Technol 30(5):438–453

Donaldson K, Li XY, Macnee W (1998) Ultrafine (nanometre) particle mediated lung injury. J Aerosol Sci 29(5–6): 553–560

Donaldson K, Stone V, Gilmour PS, Brown DM, Macnee W (2000) Ultrafine particles: mechanisms of lung injury. Philos Trans R Soc A 358(1775):2741–2749

Fierz M, Kaegi R, Burtscher H (2007a) Theoretical and experimental evaluation of a portable electrostatic TEM sampler. Aerosol Sci Technol 41(5):520–527

Fierz M, Vernooij MGC, Burtscher H (2007b) An improved low-flow thermodenuder. J Aerosol Sci 38(11):1163–1168

Gehrig R, Hill M, Lienemann P, Zwicky CN, Bukowiecki N, Weingartner E, Baltensperger U, Buchmann B (2007) Contribution of railway traffic to local PM10 concentrations in Switzerland. Atmos Environ 41(5):923–933

Gold RE, Holcslaw T, Tupy D, Ballard JB (1984) Dermal and respiratory exposure to applicators and occupants of residences treated with dichlorvos (DDVP). J Econ Entomol 77(2):430–436

Helland A, Wick P, Koehler A, Schmid K, Som C (2007) Reviewing the environmental and human health knowledge base of carbon nanotubes. Environ Health Perspect 115(8):1125–1131

Hueglin C, Gehrig R, Baltensperger U, Gysel M, Monn C, Vonmont H (2005) Chemical characterisation of PM2.5, PM10 and coarse particles at urban, near-city and rural sites in Switzerland. Atmos Environ 39(4):637–651

Kaegi R, Gasser P (2006) Application of the focused ion beam technique in aerosol science: detailed investigation of selected, airborne particles. J Microsc 224(2):140–145

Kaiser JP, Wick P, Manser P, Spohn P, Bruinink A (2008) Single walled carbon nanotubes (SWCNT) affect cell physiology and cell architecture. J Mater Sci 19(4): 1523–1527

Kaiser JP, Krug HF, Wick P (2009) Nanomaterial cell interactions: how do carbon nanotubes affect cell physiology? Nanomedicine 4(1):57–63

Keskinen J, Pietarinen K, Lehtimaeki M (1992) Electrical low pressure impactor. J Aerosol Sci 23(4):353–360

Kirchner U, Scheer V, Vogt R, Kaegi R (2009) TEM study on volatility and potential presence of solid cores in nucleation mode particles from diesel powered passenger cars. J Aerosol Sci 40(1):55–64

Knutson EO, Whitby KT (1975) Aerosol classification by electric mobility: apparatus, theory, and applications. J Aerosol Sci 6(6):443–451

Kreyling WG, Semmler-Behnke M, Mueller W (2006) Ultrafine particle–lung interactions: does size matter? J Aerosol Med 19(1):74–83

Lehmann U, Mohr M, Schweizer T, Ruetter J (2003) Number size distribution of particulate emissions of heavy-duty engines in real world test cycles. Atmos Environ 37(37):5247–5259

Leppard GG (2008) Nanoparticles in the environment as revealed by transmission Electron microscopy: detection, characterisation and activities. Curr Nanosci 4(3):278–301

Lienemann CP, Heissenberger A, Leppard GG, Perret D (1998) Optimal preparation of water samples for the examination of colloidal material by transmission electron microscopy. Aquat Microb Ecol 14(2):205–213

Limbach LK, Wick P, Manser P, Grass RN, Bruinink A, Stark WJ (2007) Exposure of engineered nanoparticles to human lung epithelial cells: influence of chemical composition and catalytic activity on oxidative stress. Environ Sci Technol 41(11):4158–4163

Liu BYH, Whitby KT, Yu HHS (1967) Electrostatic aerosol sampler for light and electron microscopy. Rev Sci Instrum 38(1):100–102

Llewellyn DM, Brazier A, Brown R, Cocker J, Evans ML, Hampton J, Nutley BP, White J (1996) Occupational exposure to permethrin during its use as a public hygiene insecticide. Ann Occup Hyg 40(5):499–509

Lorenzo R, Kaegi R, Gehrig R, Grobety B (2006) Particle emissions of a railway line determined by detailed single particle analysis. Atmos Environ 40(40):7831–7841

Morrow PE, Mercer TT (1964) A point-to-plane electrostatic precipitator for particle size sampling. Am Ind Hyg Assoc J 25:8–14

Nel A, Xia T, Maler L, Li N (2006) Toxic potential of materials at the nanolevel. Science 311(5761):622–627

Nurkiewicz TR, Porter DW, Hubbs AF, Cumpston JL, Chen BT, Frazer DG, Castranova V (2008) Nanoparticle inhalation augments particle-dependent systemic microvascular dysfunction. Part Fibre Toxicol 5:1

Oberdoerster G, Oberdoerster E, Oberdoerster J (2005) Nanotoxicology: an emerging discipline evolving from studies of ultrafine particles. Environ Health Perspect 113(7):823–839

Oberdoerster G, Stone V, Donaldson K (2007) Toxicology of nanoparticles: a historical perspective. Nanotoxicology 1(1):2–25

Olfert JS, Kulkarni P, Wang J (2008) Measuring aerosol size distributions with the fast integrated mobility spectrometer. J Aerosol Sci 39(11):940–956

Rothen-Rutishauser BM, Kiama SC, Gehr P (2005) A three-dimensional cellular model of the human respiratory tract to study the interaction with particles. Am J Respir Cell Mol Biol 32(4):281–289

Rothen-Rutishauser B, Muehlfeld C, Blank F, Musso C, Gehr P (2007) Translocation of particles and inflammatory responses after exposure to fine particles and nanoparticles in an epithelial airway model. Part Fibre Toxicolo 4:9

Sioutas C, Abt E, Wolfson JM, Koutrakis P (1999) Evaluation of the measurement performance of the scanning mobility particle sizer and aerodynamic particle sizer. Aerosol Sci Technol 30(1):84–92

Straube EKE, Bradatsch M (2000) Untersuchungen zur Bewertung der externen Belastung durch Pflanzenschutz- und Schädlingsbekämpfungsmittel beim beruflichen Einsatz im Freiland und in geschlossenen Räumen sowie zur Beanspruchung des Menschen. Aufl. 2. Greifswald: Druckhaus Panzig 1998, 98

The Royal Society (2004) Nanoscience and nanotechnologies: opportunities and uncertainties, vol 1. Science Policy Section, The Royal Society, London, p 127

Ulrich A, Wichser A (2003) Analysis of additive metals in fuel and emission aerosols of diesel vehicles with and without particle traps. Anal Bioanal Chem 377(1):71–81

Van Gulijk C, Marijnissen JCM, Makkee M, Moulijn JA (2000) Evaluation of the ELPI for diesel soot measurements. J Aerosol Sci 31(suppl 1):394–395

Vernez D, Bruzzi R, Kupferschmidt H, De-Batz A, Droz P, Lazor R (2006) Acute respiratory syndrome after inhalation of waterproofing sprays: a posteriori exposure-response assessment in 102 cases. J Occup Environ Hyg 3(5):250–261

Viana M, Kuhlbusch TAJ, Querol X, Alastuey A, Harrison RM, Hopke PK, Winiwarter W, Vallius M, Szidat S, Prevot ASH, Hueglin C, Bloemen H, Wahlin P, Vecchi R, Miranda AI, Kasper-Giebl A, Maenhaut W, Hitzenberger R (2008) Source apportionment of particulate matter in Europe: a review of methods and results. J Aerosol Sci 39(10):827–849

Wick P, Manser P, Spohn P, Bruinink A (2006) In vitro evaluation of possible adverse effects of nanosized materials. Physica Status Solidi B Basic Res 243(13):3556–3560

Wick P, Manser P, Limbach LK, Dettlaff-Weglikowska U, Krumeich F, Roth S, Stark WJ, Bruinink A (2007) The degree and kind of agglomeration affect carbon nanotube cytotoxicity. Toxicol Lett 168(2):121–131